Spatial Distribution of Energy Dissipation by High-Energy X-Rays*

HENRY BRYSK†
National Bureau of Standards, Washington, D. C.
(Received May 27, 1954)

The space distribution of energy dissipated by betatron x-rays results from the combined propagation of the x-rays and of their secondary electrons. This distribution has been calculated for a 40-Mev bremsstrahlung spectrum incident on a mass of water. The calculation is described and the results are compared with related experiments.

I. INTRODUCTION

WHEN an x-ray beam passes through a medium, it dissipates energy by ionization and excitation of the atoms. At depths in the medium greater than the range of secondary electrons, the different forms of radiation are, to a considerable extent, in equilibrium with each other and the energy dissipation follows approximately the x-ray spatial distribution, slightly displaced forward because of electron travel. Close to the entrance surface in the medium, on the other hand, there is little energy dissipation because the x-rays have not yet had much chance to produce secondary electrons which in turn dissipate the energy. Hence, the energy dissipation rises from a low value at the surface to a maximum further in (transition curve), then falls off with the x-ray distribution.

The transition curve is of considerable radiological interest because the energy dissipation is a measure of the biological effect. The position of the maximum depends on the x-ray energy and attains depths of the order of 1–10 cm for x-rays from multimillion volt accelerators. In medical applications requiring irradiation at a spot inside the body, it may be desirable to select a source such that the maximum of the transition curve will fall on the target, so as to minimize unnecessary irradiation of other areas. A certain number of measurements of transition curves have been made in the multimillion volt range[1] but there has been no previous attempt to perform a detailed theoretical calculation which takes into account the penetration, degradation, and diffusion of the x-rays and of their secondary electrons.

The equations that govern this phenomenon lend themselves to a straightforward calculation of the moments of the distribution of radiation, provided that the boundary effects can be schematized in the following manner: the x-ray beam will be assumed to be generated at the position of the entrance surface and to be perpendicular to the surface. The medium will be assumed to extend over all the space, even behind the entrance surface. The analytical transformations required to derive the moments have been given by Lewis[2] for electrons and by Spencer and Fano[3] for x-rays. For x-rays it has also been possible to utilize the values of a few moments and a rough knowledge of the trend of penetration to give a rather accurate description of the whole x-ray distribution.[3] Efforts to achieve the same results for the distribution of electrons derived from a collimated electron beam have not yet been successful. However, the combined penetration of x-rays and secondary electrons, which gives rise to the transition curve, offers a somewhat easier problem because the deep penetration is controlled by the x-rays rather than by the electrons. The solution of this problem for a typical example is reported in the present paper.

If the energy of the incident x-rays (or of incident electrons) is sufficiently high the electrons generate a large amount of bremsstrahlung and the bremsstrahlung a large amount of high-energy pair electrons which yield more bremsstrahlung. The transition curve goes over, then, into a shower curve. The work reported here concerns a combination of source energy and medium for which the bremsstrahlung of secondary electrons represents a minor effect which has been disregarded. The detailed calculation of a shower process would be only a little more complicated in principle and moderately more laborious in practice; it represents the next logical step in the program of this laboratory.

The experimental arrangement corresponding to the calculation described here is the following: A beam of 40-Mev electrons strikes a thin tungsten target in a betatron. Electrons leaving the target are removed (magnetically) and the (collimated) bremsstrahlung beam enters a tank of water. The calculation predicts the energy dissipation in a plane section, perpendicular to the direction of travel of the incident radiation, as a function of penetration distance in the water.

The calculation is accomplished in four stages: (1) spatial moments of the x-ray distribution resulting from scattering and absorption of the incident x-rays are calculated by the method of reference 3; (2) these moments are then used to calculate the spatial moments

* Work supported by the Office of Naval Research and the U. S. Atomic Energy Commission.
† Now at Oak Ridge National Laboratory, Oak Ridge, Tennessee.
[1] See, e.g., Koch, Kerst, and Morrison, Radiology **40**, 120 (1943). E. E. Charlton and H. E. Breed, Am. J. Roentgenol. Radium Therapy **60**, 158 (1948). Johns, Darby, Haslam, Katz, and Harrington, Am. J. Roentgenol. Radium Therapy **62**, 257 (1949). Laughlin, Beattie, Lindsay, and Harvey, Am. J. Roentgenol. Radium Therapy **65**, 787 (1951).
[2] H. W. Lewis, Phys. Rev. **78**, 526 (1950).
[3] L. V. Spencer and U. Fano, J. Research Natl. Bur. Standards **46**, 446 (1951).

of the electron and positron distribution which is produced directly by the x-rays through Compton scattering and pair production; (3) the moments resulting from (2) are used as the source in an electron diffusion equation the solution of which yields spatial moments of the electron distribution at various stages in the slowing-down process[2]; and (4) the moments resulting from (3) are used to construct the spatial distribution of electrons of each energy from which the energy dissipation as a function of depth is directly calculated.

It should be noted that the method of calculation affords the convenience of proceeding from one set of moments to the next, without actually reconstructing detailed spatial distributions until the final stage of the calculation.

II. X-RAY DIFFUSION

The spectrum of x-rays emerging from a betatron is not known in detail; however, the spectrum given by Bethe and Heitler[4] (or that of Schiff,[5] which is essentially the same) is believed to be reasonably accurate.[6] We assumed the (40-Mev) source spectrum striking the plane water barrier (perpendicularly) to be of this form.

Considering the integral of the radiation over an infinite plane perpendicular to the incident radiation renders the problem one-dimensional in space. This is equivalent to considering diffusion from a plane monodirectional source which is laterally infinite in extent. The diffusion equation for this situation is reduced in reference 3 to a set of interlinked integral equations. The solutions of these integral equations yield Legendre-Laguerre coefficients H_{ln} which are defined as follows:

$$H_{ln}(k)=\int dz L_n(\alpha z)\int_{4\pi} d\Omega P_l(\cos\theta)H(k,\theta,z), \quad (1)$$

where k is the photon energy in mc^2 units, θ is the angle between the photon direction and the direction of incidence, z is distance of the photon from the incident plane, α is a parameter which we take to be the narrow-beam attenuation coefficient of the 40-Mev radiation component, and $H(k,\theta,z)$ is the x-ray distribution function. P_l and L_n are the Legendre and Laguerre polynomials of the lth and nth degree, respectively.

It should be noted that the use of Laguerre coefficients instead of moments represents a convenience without loss of generality; the nth Laguerre coefficient is a linear combination of the first n moments and vice versa. (See Sec. V for further discussion.)

Our first objective was the calculation of H_{ln} for $l, n \leq 3$. This was accomplished by solving ten of the integral equations given in expression (10) of reference 3. The attenuation coefficients used were those of White[7]; and, as discussed at the beginning of this section, the source spectrum was that of Schiff. Straightforward numerical techniques were used, a detailed discussion of which can be found in a report by Berger and Doggett.[8] The solutions were carried to the lowest energy of x-rays which can give rise to electrons with 1 mc^2 kinetic energy (see Sec. III).

III. ELECTRON SOURCE

The next step in the calculation is to determine the Legendre-Laguerre coefficients of the electrons which are generated by the x-rays. We designate the distribution of these secondary electrons by $G(E,\theta,z)$ and write down the expression which relates $G(E,\theta,z)$ to the x-ray distribution $H(k,\theta,z)$, namely,

$$G(E,\theta,z)=\int dk\int d\Omega' p(k,E,\Theta)H(k,\theta',z), \quad (2)$$

where $p(k,E,\Theta)$ is the probability per unit photon path length per unit solid angle that a photon with energy between k and $k+dk$ produces an electron (or positron) of kinetic energy E traveling at an angle Θ with the photon direction. The integral over k includes all photon energies capable of producing an electron of energy E.

It is easy to see that (2) implies a similar relation between the Laguerre coefficients:

$$G_n(E,\theta)=\int dk\int d\Omega' p(k,E,\Theta)H_n(k,\theta'). \quad (3)$$

Further, by using the addition theorem of spherical harmonics, one obtains a convenient relation between the Legendre-Laguerre coefficients of G and H:

$$G_{ln}(E)=\int dk p_l(k,E)H_{ln}(k), \quad (4)$$

where

$$G_{ln}(E)=\int dz L_n(\alpha z)\int d\Omega P_l(\cos\theta)G(E,\theta,z),$$
$$p_l(k,E)=\int d\Omega P_l(\cos\theta)p(k,E,\theta). \quad (5)$$

Electrons of kinetic energy 1 mc^2 have a range of about 1 mm in water. Electrons of lower energy than this will be considered to lose all their energy at the point of origin. We, therefore, want to calculate $G_{ln}(E)$ only for $E \geq 1$ mc^2. The processes which are effective in water in yielding electrons with such energies are pair production and recoil from Compton scattering.

The cross section per atom for recoil from Compton scattering (in units of the Thomson cross section) can

[4] H. Bethe and W. Heitler, Proc. Roy. Soc. (London) **146**, 83 (1934).
[5] L. I. Schiff, Phys. Rev. **83**, 252 (1951).
[6] H. W. Koch and R. E. Carter, Phys. Rev. **75**, 1950 (1949).
[7] G. R. White, Natl. Bur. Standards Rept. 1003 (unpublished).
[8] M. J. Berger and J. A. Doggett, Natl. Bur. Standards Rept. 2224 (unpublished).

be obtained from the Klein-Nishina formula[9]:

$$\sigma^{KN}(k,E,Z) = \frac{3Z}{4}\frac{1}{k^2}\left\{1+\frac{E}{2k(k-E)}\left[(E-2)+\frac{E}{k(k-E)}\right]\right\}, \quad (6)$$

where the energies are expressed in mc^2 units and Z is the nuclear charge. In the Compton effect, fixing k and E also fixes the angle of scattering:

$$\cos\Theta = \frac{1+k}{k}\left(\frac{E}{E+2}\right)^{\frac{1}{2}}. \quad (7)$$

Hence

$$\sigma^{KN}(k,E,\Theta,Z) = (2\pi)^{-1}\sigma^{KN}(k,E,z)\delta\left[\cos\Theta-\frac{1+k}{k}\left(\frac{E}{E+2}\right)^{\frac{1}{2}}\right], \quad (8)$$

where δ is the Dirac delta function, and finally

$$\sigma_l^{KN}(k,E,Z) = \sigma^{KN}(k,E,z)P_l\left[\frac{1+k}{k}\left(\frac{E}{E+2}\right)^{\frac{1}{2}}\right], \quad (9)$$

where

$$0 \leq \frac{1+k}{k}\left(\frac{E}{E+2}\right)^{\frac{1}{2}} \leq 1.$$

For pair production, in water, at the range of energies of interest, the unscreened Born approximation as calculated by Bethe and Heitler[4] is adequate. The expression for the angular distribution[10] is, however, quite cumbersome and its Legendre expansion[11] is unwieldy. Fortunately, high-energy pair electrons are mostly produced within a cone of about angle $1/E$ with respect to the incident photon direction. This means that the coefficients of the Legendre expansion of the cross section tend to decrease in size quite slowly with l. Since we only need the first few coefficients, we assume for simplification that these coefficients are all equal, i.e., given by the Bethe-Heitler expression[4] integrated over all directions.

All coefficients would be equal if the electrons were generated traveling in the direction of the pair-producing photon. For low-energy electrons, the range is small and therefore the directional assumption is unimportant. A simple calculation indicates that the above approximation never displaces electrons more than about 1 mm from their true position.

We found it convenient to use Hough's simplified forms for the unscreened Bethe-Heitler cross section.[12] These are the following (in units of the Thomson cross section): For $k \geq 15$,

$$\sigma^{BH}(k,E,Z) = \frac{3}{2\pi}\frac{Z^2}{137}\frac{1}{k}\left[1-\frac{4}{3}\frac{(E+1)(k-E-1)}{k^2}\right] \times\left[\ln\frac{2(E+1)(k-E-1)}{k}-\frac{1}{2}\right], \quad (10)$$

and for $2 \leq k \leq 15$,

$$\sigma^{BH}(k,E,Z) = \frac{3}{8\pi}\frac{Z^2}{137}\Phi J\frac{1}{k-2} \times[1+0.135(\Phi-0.52)J(1-J)^2], \quad (11)$$

where

$$J = 2[x(1-x)]^{\frac{1}{2}}, \quad x = \frac{E}{k-2},$$

$$\Phi = 2.32\left(\frac{k-2}{k}\right)^2\ln\left(\frac{k}{2}\right)+A(k),$$

and $A(k)$ is a graphed correction term. The second term in the brackets of (11) is to be dropped when it becomes negative.

For our purpose no distinction need be made between electrons and positrons, since their diffusion properties do not differ appreciably in low-Z materials. The cross section for electron production should then be multiplied by two.

Pair production can also occur in the field of an electron, though it is less probable than pair production in the field of a nucleus by about a factor $(1/Z)$ at high energies. This cross section also falls off more rapidly at low energies and vanishes for $k \leq 4\ mc^2$. The angular distributions of the two kinds of pair production are closely similar.[13] We accounted for electronic pair production by increasing the nuclear pair production by 10 percent ($Z=10$). This is correct for high energies, and the overestimate at low energies is never more than 1 percent of the over-all electron-producing cross section[7] because the Compton effect then overshadows pair production from all sources.

Combining the over-all pair production cross section with the Compton recoil cross section, we have for the lth Legendre coefficient of the total probability for electron production

$$p_l(k,E) = \sum_i N_i\phi_0\sigma_l^{KN}(k,E,Z_i) + 2.2\sum_i N_i\phi_0\sigma^{BH}(k,E,Z_i), \quad (12)$$

where N_i is the number of atoms of each kind per unit volume and ϕ_0 is the Thomson cross section. In order to obtain the Legendre-Laguerre coefficients of the electron source, i.e., the G_{ln}, we entered these $p_l(k,E)$ into the integrals (4) and carried out the integration numerically.

[9] A. T. Nelms, Natl. Bur. Standards Circ. 542 (unpublished).
[10] F. Sauter, Ann. Physik (5) **20**, 404 (1934).
[11] H. Brysk, Natl. Bur. Standards Rept. 2277 (unpublished).
[12] P. V. C. Hough, Cornell report reproduced in part in Phys. Rev. **73**, 266 (1948).
[13] K. M. Watson, Phys. Rev. **72**, 1060 (1947).

IV. ELECTRON DIFFUSION

The diffusion of electrons is represented by the Lewis equation,[2] which relies on the approximation of continuous energy loss, according to which the energy of an electron at each point of its track is identified by its residual range r (i.e., by the initial range minus the path length s already traveled).[14] The Lewis equation pertinent to a problem in plane geometry is the following:

$$\left[-\frac{\partial}{\partial r}+\cos\theta\frac{\partial}{\partial z}\right]f(z,\theta,r)=(2\pi)^{-1}N\phi_0\int d\Omega'\times[f(z,\theta',r)-f(z,\theta,r)]\sigma^R(r,\Theta)+g(z,\theta,r), \quad (13)$$

where $f(z,\theta,r)$ is the distribution function and $g(z,\theta,r)$ is the source function. The corresponding Legendre-Laguerre coefficient equations are

$$-\frac{\partial}{\partial r}f_{ln}(r)+\frac{\alpha}{2l+1}\sum_{m=0}^{n-1}[(l+1)f_{l+1,m}(r)+lf_{l-1,m}(r)]=-k_l(r)f_{ln}(r)+g_{ln}(r), \quad (14)$$

where $k_l(r)=N\phi_0[\sigma_0{}^R(r)-\sigma_l{}^R(r)]$, and α is the scale factor already mentioned. Lewis obtains formally closed solutions of these equations in terms of the quantity $\exp\{-\int k_l(r)dr\}$. However, the integral cannot be performed analytically, and it turns out to be computationally simpler to convert the differential equations into Volterra integral equations of the second kind. These integral equations are similar to those in the gamma-ray diffusion problem and can be solved numerically in an analogous manner. We integrate (14) over the residual range from r to ∞. Since f is zero at the upper limit,

$$f_{ln}(r)=-\frac{\alpha}{2l+1}\sum_{m=0}^{n-1}\left[(l+1)\int_r^\infty f_{l+1,m}(r')dr'+l\int_r^\infty f_{l-1,m}(r')dr'\right]-\int_r^\infty k_l(r')f_{ln}(r')dr'+\int_r^\infty g_{ln}(r')dr'. \quad (15)$$

Changing over from residual range to energy as the variable for convenience we set

$$f_{ln}(r)dr=F_{ln}(E)dE,\quad g_{ln}(r)dr=G_{ln}(E)dE,\quad k_l(r)dr=K_l(E)dE. \quad (16)$$

Then

$$F_{ln}(E)\left(\frac{dE}{dr}\right)=-\frac{\alpha}{2l+1}\sum_{m=0}^{n-1}\left[(l+1)\int_E^\infty F_{l+1,m}(E')dE'+l\int_E^\infty F_{l-1,m}(E')dE'\right]-\int_E^\infty K_l(E')F_{ln}(E')dE'+\int_E^\infty G_{ln}(E')dE'. \quad (17)$$

For the electron scattering cross section, we used a screened Rutherford cross section with the relativistic correction in low-Z approximation[15]:

$$\sigma^R=\frac{Z(Z+1)}{p^2\beta^2}\left\{\frac{1-\beta^2\sin^2(\theta/2)}{[1-\cos\theta+2\eta]^2}\right\}. \quad (18)$$

Here the substitution of $Z(Z+1)$ for Z^2 accounts roughly for electron-electron deflections.[16] For η we used Molière's value,[17]

$$\eta=0.0000686[(1-\beta^2)/\beta^2]\times Z^{\frac{2}{3}}[1.13+3.76(Z/137\beta)^2]. \quad (19)$$

Correspondingly, we obtain for the $K_l(E)$,

$$K_l(E)=N\phi_0\tfrac{3}{4}Z(Z+1)\left\{\frac{(E+1)}{E(E+2)}\right\}^2C_l(\eta), \quad (20)$$

where

$$C_l(\eta)=\int_{-1}^{1}\frac{1-\beta^2\sin^2(v/2)}{(1-\cos\theta+2\eta)^2}[1-P_l(\cos\theta)]d(\cos\theta). \quad (21)$$

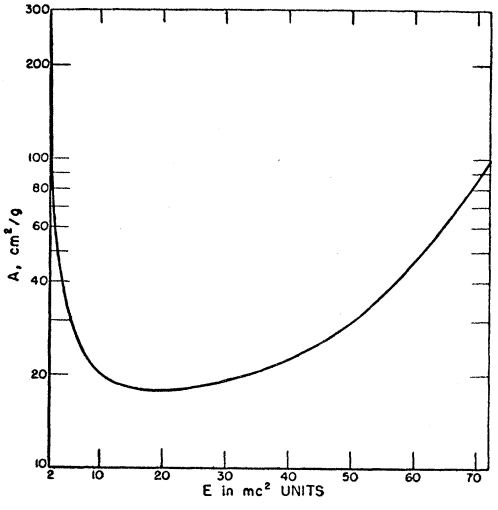

FIG. 1. The parameter A, whose reciprocal indicates the thickness required to bring electrons of different energies to equilibrium with the γ-ray spectrum.

[14] Lewis uses s as variable for an electron of given initial energy. For electrons of different initial energies, s no longer uniquely determines the energy, but r does—hence our modification.

[15] N. F. Mott and H. S. W. Massey, *The Theory of Atomic Collisions* (Oxford University Press, London, 1949), second edition, p. 80.

[16] This point was obtained in detail by Fano while the work was in progress [U. Fano, Phys. Rev. **93**, 117 (1954)]. The $Z(Z+1)$ approximation represents an underestimate of σ^R of the order of 4 percent. The error introduced in the final result is of course much less.

[17] G. Molière, Z. Naturforsch. **2a**, 133 (1947).

In the limit $l \leq \eta^{-1}$, which is obviously satisfied for all l's of interest, the integral becomes[18]

$$C_l(\eta) = \tfrac{1}{2} l(l+1)(1-\ln\eta - 2\sum_{m=1}^{l} m^{-1}) - \beta^2 \sum_{m=1}^{l} m^{-1}. \quad (22)$$

For the stopping power we used

$$\frac{dE}{dr} = \tfrac{3}{4} N\phi_0 Z \frac{(E+1)^2}{E(E+2)} B, \quad (23)$$

where the stopping number B is given by[19]

$$B = \ln[E^2(E+2)] - [1+(2E+1)/(E+1)^2]\ln 2 + (E+1)^{-2} + 2\ln\left(\frac{mc^2}{I}\right) - \delta. \quad (24)$$

The last two terms are taken from Sternheimer.[20]

Using these functions and the ten $G_{ln}(E)$ from the preceding stage of the calculation, we solved the corresponding ten equations (17) by standard numerical methods.

V. CONSTRUCTING THE DISTRIBUTION OF ELECTRONS

The calculations so far have been carried out in terms of Legendre-Laguerre coefficients. We now wish to use these coefficients to construct the distribution. The conceptual basis of the procedure is discussed in reference 3. In brief, we represent the distribution as the product of a weight function and a sum of polynomials orthonormal with respect to the weight function. The success of the procedure depends upon finding a weight function for which the polynomial series converges rapidly. This implies that the weight function bears sufficient resemblance to the actual distribution.

For the gamma-ray problem the distribution is basically exponential. The weight function can be chosen to be $\exp(-\mu_0 z)$, where μ_0 is the attenuation coefficient of the 40-Mev component of the radiation. The orthonormal polynomials are then the Laguerre polynomials $L_n(\mu_0 z)$.

For the electron distributions, our general knowledge of the shape of the transition curve led us to select a weight function of the form[21]

$$W(A,z) = e^{-\mu_0 z} - e^{-A\mu_0 z}. \quad (25)$$

[18] See reference 2, e.g., extended by C. H. Blanchard (private communication).

[19] H. Bethe, *Handbuch der Physik* (Springer, Berlin, 1933), Vol. 24, No. 1, p. 523.

[20] R. M. Sternheimer, Phys. Rev. **88**, 851 (1952).

[21] H. E. Johns *et al.*, Am. J. Roentgenol. Radium Therapy **62**, 257 (1949), have assumed that the energy dissipation is distributed in this manner on the basis of a qualitative picture of energy propagation as a two-step decay process. Since electron penetration does not follow a simple exponential law, this line of thought is not as convincing as one would like.

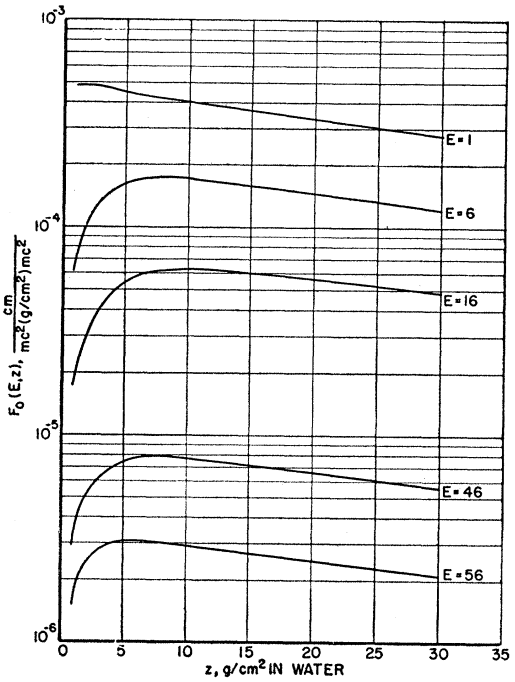

FIG. 2. The number flux of electrons as a function of z for various electron energies. $F_0(E,z)$ is expressed in units of track length (cm) per unit electron kinetic energy (mc^2) per unit thickness of medium (g/cm²) per unit incident γ-ray energy (mc^2).

To construct the spatial distribution of electrons of a given energy E, we constructed the orthonormal polynomials $w_n(A,z)$ associated with $W(A,z)$, and determined the coefficients $a_n(A,E)$ of the expansion $F_0(E,z) = W(A,z)\sum_n a_n(A,E) w_n(A,z)$, for $n=0$, 1, 2, 3, so that the distribution had the calculated values of F_{00}, F_{01}, F_{02}, and F_{03}.

For reasonable values of A, the $a_n(A,E)$ converged rapidly, so that the criterion for selecting A could be taken to be $a_3(A,E)=0$. Using this criterion, A's were obtained for different electron energies. Figure 1 shows a plot of A's so determined as a function of electron energy. The value of A affords a gauge of the departure of electron distributions from the gamma-ray distribution. For high-electron energies A is very large, signifying that electrons of these energies cannot, on the average, have traveled far from their point of origin. (Large path lengths mean large energy losses, which these electrons have obviously not undergone.) For low electron energies, A is again large, signifying that many of these electrons were produced with so little energy that they could not stray far from their point of origin. The electron energies slowest to come to equilibrium with the gamma rays (smallest values of A) are those of intermediate energies.

The behavior of A as a function of E and the numerical values for A are quite reasonable. We therefore gained some confidence in the fitting procedure and evaluated the polynomial sums representing electron

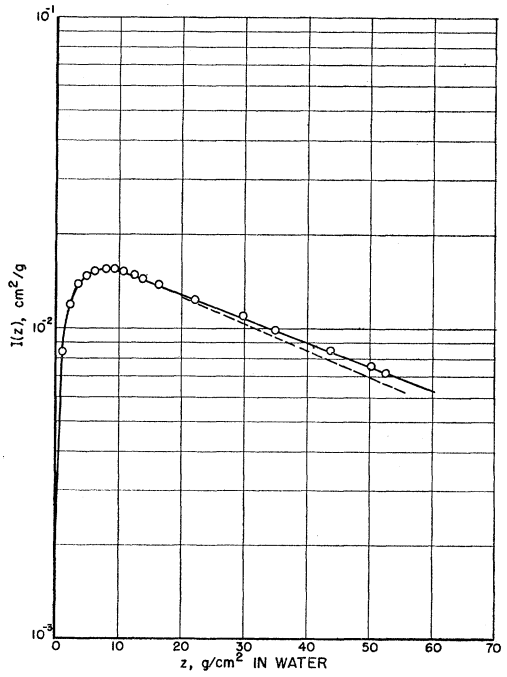

FIG. 3. The fraction of the incident γ-ray energy dissipated per unit thickness (g/cm^2). The solid line is the theoretical energy dissipation distribution. The circles represent the measurements of Zendle and Koch corrected to include off-axis radiation. The dashed line represents the uncorrected Zendle-Koch data (normalized to agree with the theoretical value at the peak of the transition curve).

space distributions for each electron energy and for selected z's. Figure 2 shows the number of electrons as a function of z for various electron energies.

The energy dissipated by electrons of each energy E is obtained by weighting the number of electrons having energy E with the stopping power (dE/dr). The total energy dissipated at z is then given by the expression $I(z)=\int F_0(E,z)(dE/dr)dE$.[22] We evaluated these integrals for several values of z. The resulting distribution is shown in Figs. 3 and 4.

Figure 5 shows the electron spectra at several depths z. The quantity plotted is for convenience $(E/\beta)\times e^2F_0(E,z)$, and is proportional to the density of energy carried by electrons of energy E because $F_0(E,z)$, a flux, is proportional to the velocity β.

VI. CORRECTIONS AND CHECKS

A number of minor approximations were made in the course of performing the calculations which will be discussed in this section. Internal checks in the calculation are also mentioned briefly.

[22] Note that $F_0(E,z)$ has dimensions track length per unit thickness of medium per unit electron energy; per unit incident γ-ray energy so that $I(z)$ is the fraction of the incident energy dissipated per unit thickness. The integral $\int_0^\infty I(z)dz$ must therefore be unity. For a discussion of the units of the space integral of $F_0(E,z)$ see U. Fano, Phys. Rev. **92**, 328 (1953), or L. V. Spencer and U. Fano, Phys. Rev. **93**, 1172 (1954).

The detailed calculations described in the preceding sections were performed for electrons with kinetic energies greater than 1 mc^2 and for x-rays with photon energies sufficient to give rise to electrons with such energies ($k>1.37$ mc^2). Electrons with kinetic energies lower than 1 mc^2, which are not penetrating and do not dissipate a large fraction of the total energy input, were treated in a cruder approximation. These low-energy electrons arise in several ways, namely:

(1) from source x-rays with energies below the "threshold" adopted for the detailed calculation or from x-rays achieving an energy below "threshold" through Compton scattering (8 percent of the total energy input),

(2) from high-energy x-rays directly by Compton recoil or pair production or from high-energy electrons which have lost most of their energy in electron diffusion (9 percent of the total energy input), and

(3) from annihilation radiation (2 percent of the total energy input).

We assumed that low-energy electrons contributed by (1) are distributed spatially exactly as are the lowest-energy *x-rays* treated in the detailed calculation of the x-ray distribution. We assumed that low-energy electrons contributed by (2) and (3) are distributed spatially like the 1 mc^2 electrons.

These assumptions should be quite adequate since low-energy x-rays and electrons tend to maintain a relative equilibrium with components of slightly higher energies. One may question whether this is the best way to treat annihilation radiation, which has an additional fairly large path length after the positrons are stopped. However, annihilation radiation represents only about 2 percent of the input energy and since the

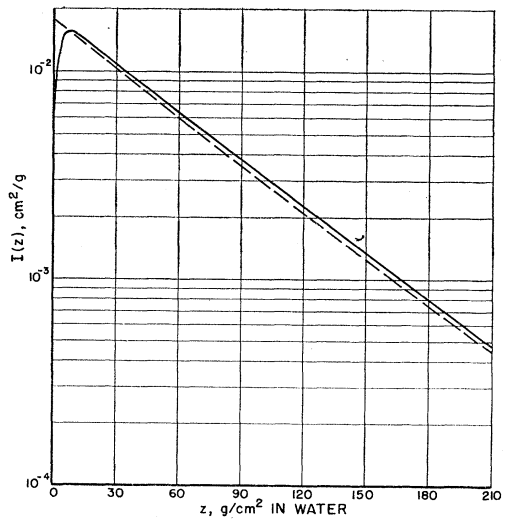

FIG. 4. A comparison between the energy dissipation curve $I(z)$ (solid line) and the energy dissipation curve calculated as if the electrons deposited their kinetic energy precisely where they are generated.

annihilation photons travel in opposite directions the "center of mass" of the radiation remains at the end of the positron range.

In order to determine the amount of energy contributed by (1), (2), and (3), we calculated the total energy generated in the form of x-rays or electrons above "threshold" at each stage of the calculation and made comparisons with the total input energy. This comparison of total energies generated at each stage of the calculation serves as an excellent internal check on the accuracy of the calculations.

Bremsstrahlung from the electrons was neglected because (a) the cross section is small because of the low atomic number of the medium, (b) the electron spectrum is strongly peaked at low energies, and (c) the bremsstrahlung cross section is also peaked at low energies.

The boundary would influence the x-ray calculation only for photons below 200 kev.[23] In the electron part of the calculation, low-energy electrons quite near the boundary would be affected. However, these are few—the electron distribution builds up from near zero at the boundary.

Inasmuch as this was a pilot calculation, many detailed considerations were included which represent refinements considerably beyond the accuracy required for the particular result. A discussion of the simplifications that can be made for a limited objective—and their justification—will be presented in a subsequent paper.

VII. COMPARISON WITH EXPERIMENT

An accurate experimental determination of the ionization depth dose of a betatron beam in water *along the axis of the beam* was made by Zendle and Koch.[24] On the other hand, the theoretical calculation is for the energy loss over the entire plane perpendicular to the direction of motion. To obtain the latter quantity, Boag and Zendle[25] complemented the Zendle-Koch results by measurements with annular beams. An *absolute* calibration of the experimental results was achieved. Figure 3 presents the theoretical transition curve (also absolute) together with the final experimental points. It is seen that excellent agreement is obtained both as to absolute intensities and variation with depth. For comparison (and caution), Fig. 3 also includes some of the Zendle-Koch data—the deviation is essentially due to the fact that in the latter case the crystal does not see radiation scattered away from the central axis. Figure 4 compares the depth variation (found for the energy loss) of the calculated energy dissipation with that which would result from a gamma-ray calculation disregarding electron travel. The two curves are seen to be parallel at greater depths, the correct curve being displaced some 4–5 cm deeper into the medium.

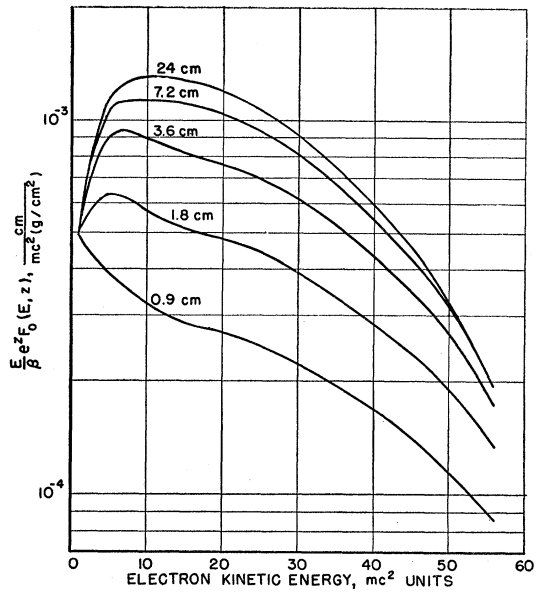

FIG. 5. Electron spectra at various depths z.

The interpretation of the electron spectra in Fig. 5 follows: The spectrum very near $z=0$ represents electrons immediately after their production by the x-rays. On the other hand, at 24 cm the electron spectrum has reached an equilibrium state which changes only as the x-ray spectrum changes, i.e., very slowly. The transition is characterized by an increase in the energy density carried by electrons of intermediate energies, which may be produced not only directly from the x-rays but by the slowing down of higher energy electrons.

The confluence of all curves on the left side seems to be accidental. The elementary calculation of electron spectra by Cormack and Johns[26] pertains in fact to zero depth, and the curve labeled "betatron" in their Fig. 7 resembles the 0.9-cm curve in Fig. 5 of this paper.

ACKNOWLEDGMENTS

This work was closely related to previous research and experience of members of the Nuclear Physics Section of the National Bureau of Standards, and the extent of their contributions is only partly reflected in the references. I wish to thank my colleagues M. J. Berger, C. H. Blanchard, U. Fano, L. V. Spencer, and G. R. White for many fruitful discussions. I am indebted to J. A. Doggett for the computation of the A values and for the figures. Access to the data of J. W. Boag, H. W. Koch, and B. Zendle of the Betatron Section in advance of publication was greatly appreciated. L. V. Spencer kindly undertook the unpleasant task of editorial review of the manuscript.

[23] M. J. Berger (private communication).
[24] B. Zendle and H. W. Koch (private communication).
[25] J. W. Boag and B. Zendle (private communication).
[26] D. V. Cormack and H. E. Johns, Brit. J. Radiol. **25**, 369 (1952).